International Journal of Emerging Engineering and Technology (IJEET)
ISSN (e): 2958-3764
Volume: 5, Number: 1-2, Pages: 82 - 88, Year: 2026 (Special Issue)

Performance Evaluation of Grey Wolf Optimizer and Genetic Algorithm Tuned Controllers for Stabilizing a Hybrid Nanogrid

Saima Akram[1], Safdar Raza[1], Linta Khalil[1,*], Muhammad Kamran Liaqat Bhatti[1], Kiran Khalil[2], and Rabbia Siddique[1]

[1]Department of Electrical Engineering, NFC Institute of Engineering & Technology, Multan, 60000, Pakistan
[2]Department of Electrical Engineering, Bahauddin Zakariya University, Multan, Pakistan
[*]Corresponding author: Linta Khalil (Email: khalillinta@gmail.com)

Received: 25/09/2026, Revised: 18/11/2026, Accepted: 21/11/2026

***Abstract*—Our country, Pakistan, is now coping with several challenges. Electric power is one of them. Therefore, it is necessary to provide these resources to address power problems. To continuously supply electricity to a load, a hybrid nano grid integrates renewable and non-renewable energy sources in an eco-friendly, self-sufficient manner. The rising complexity of the power system necessitates the design of an appropriate controller. This work introduces various controllers, such as Proportional-Integral-Derivative (PID), Fractional-Order Proportional-Integral-Derivative (FOPID) and Sliding Mode Control (SMC), to minimize power oscillations caused by generation sources and load disturbances and maintain the stability of the nano-grid system. The Grey Wolf Optimization (GWO) and genetic algorithm (GA) techniques are used to determine the PID, FOPID, and SMC controllers' optimal gains using MATLAB software. The integral square error serves as the objective function in both optimization techniques. In terms of power stability, SMC has done better than any other optimized controller. When applied to every controller, the GWO method has proven to be more effective than the Genetic Algorithm (GA) technique.**

***Index Terms*— Hybrid Nano Grid System, PV Array, Wind Turbine, Fuel Cell, Genetic Algorithm (GA), Grey Wolf Optimization (GWO).**

I. INTRODUCTION

For the alleviation of environmental issues brought on by excessive non-renewable use, power systems employ renewable resources. However, overuse and infrastructure expansion pose challenges, including faulty equipment and line losses due to uncontrolled power consumption from the conventional grid [1]. The majority of the 1.2 billion population, mostly in isolated settlements, often find connecting to the power grid impractical due to societal, ecological, and financial issues [2]. A feasible answer to the aforementioned issues is the implementation of Nano-grid technology, which functions as an autonomous power system. Its compact size and capacity (15-70 kW) make it ideal for electrically isolated regions. Nano-grids support both DC and AC power, relying on electronic converters to efficiently harness and transfer energy [3]. The main challenge in managing a Nano-grid is ensuring power stability amidst fluctuating renewable sources, which can be achieved through source-side and load-side control techniques [4].

In [5], convex programming and the Keating controller are utilized in a hybrid nano-grid that is powered by solar-battery technology for the efficient management of power for areas with local loads. The design of Photovoltaic and battery sources in conjunction with demand-side management and a smart inverter-based nano-grid is the main emphasis of [6]. A DC load can be supplied by a hybrid nano-grid that uses both renewable and non-renewable power sources, with the help of an LLC-based DC converter in [7]. In addition, a study was published in [8] that provided precise power sharing in a distributed DC nano-grid with a balanced battery state of charge. In [9], a linear quadratic regulator controller with the goals of optimizing power management and guaranteeing transient stability of a DC nano-grid powered by an open photovoltaic source has been proposed. Using V2G technology, a PV-based nano-grid was created to control power flow [10]. Reference [11] designs a hybrid microgrid using a photovoltaic source, using PI and PID switches for active power regulation. The hybrid microgrid in [12] utilizes PI and PID switches for active power regulation, utilizing frequency-based control strategies to manage both demand and source sides. Binary and real-coded genetic algorithms are used in a fuel cell-powered DC nano grid system to optimize the PID controller to achieve power stability in [13]. For a multi-nano grid system, an adaptive multi-agent-based control technique is used to control the power sharing and voltage management [14].

In this paper, the hybridization of solar-wind-fuel cell systems is investigated with other optimization algorithms with different controllers to stabilize the power. The design of a 60-kW nano-grid powered by fuel cells, wind, and solar PV has been contributed in this research with Grey Wolf Optimization (GWO) with its parameter (alpha & beta) and Genetic Algorithm (GA) using FOPID, PID and SMC controllers. The suggested algorithms (GA and GWO) utilized in this study have the following advantages: they are highly flexible and reliable; they fast converge; they are easy to implement; they have strong robustness; they can handle the objective function; and they can be combined with another optimization algorithm. These algorithms are used to adjust the various controllers' parameters (PID, FOPID, and SMC,

This work is licensed under a Creative Commons AttributionShareAlike4.0 International License, which permits unrestricted use, distribution, and reproduction in any medium, provided the original work is properly cited

for example). Along with the usual controllers, a comparison is made. The ISE is the goal function that is being minimized with the help of the strategies under consideration. For the purpose of switching renewable energy resources (RERs), a switching algorithm is also introduced.

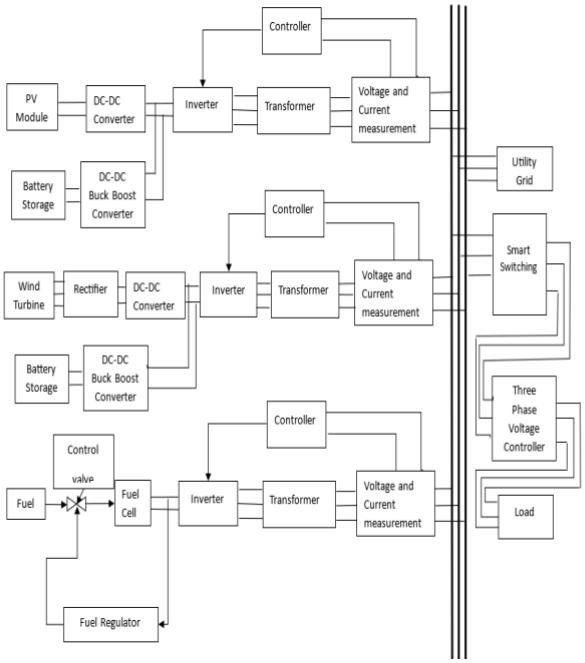


Fig. 1: Block diagram of nano-grid system [15]

This work examines the viability of producing power from renewable energy at different controllers; the first design concept is displayed in Fig. 1.

II. METHODOLOGICAL FRAMEWORK

The 60 KW nano-grid combines wind and sun energy sources and a fuel cell, producing 20 kilowatts each. Connecting occurs when load demand exceeds 60 KW, and excess power is sent to the main grid. The proposed nano-grid system effectively reduces power fluctuations due to various control techniques, utilizing genetic algorithms and grey wolf optimization method. Numerous control techniques manage reactive and active power, with a sophisticated switching algorithm alternating between renewable energy sources and the grid based on load demand. PV modules, wind turbines, and fuel cells are major sources. Price is the deciding factor when it comes to identifying the generation sources. Figure 2 shows the flow chart for the approach.

A. PV array

The PV array, consisting of 23 strings, can draw 305.226 units of power from a single cell, resulting in a 35-kW array capable of capturing 20 kW of power. The array uses MPPT technology and two converters, the Buck-Boost converter connected to storage batteries. The buck converter stores energy in batteries for PV array failure, which is then recovered by an inverter using a boost mechanism, and a DC-DC boost converter raises voltages during subsequent wing phases. Figure 3 shows the block diagram of PV array [15].

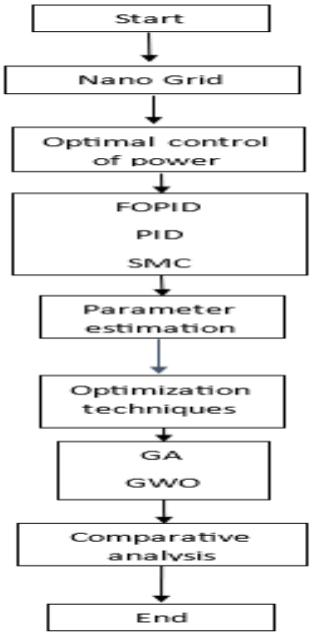


Fig. 2: Proposed design methodology

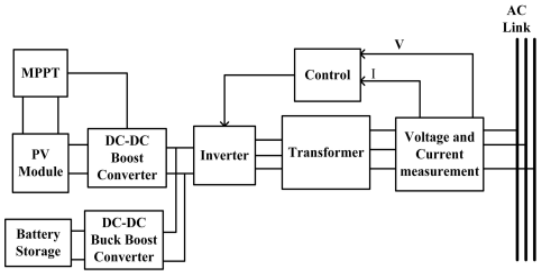


Fig. 3: PV array source wing

B. Wind turbine

The WT, connected to a nano-grid, generates 20 kW with a power factor of 0.8 and 12 kW of reactive power. Its AC output needs to be converted to DC using a Buck-Boost converter to stabilize the power supply and store it in batteries. Because of this, power can be used even when other power sources are unavailable. Block diagram of wind turbine source [15-19] is depicted in Fig. 4.

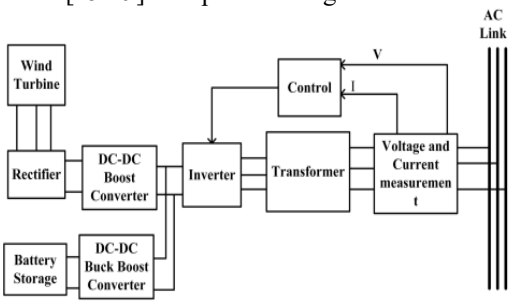


Fig. 4: Wind turbine source wing

C. Fuel Cell

Fuel cells, with rated generating capacity, can vary in generation. Governor control is used to regulate diesel engine and fuel cell generation based on load requirements. The fuel cell generates 700V DC voltage, which is fed into an inverter

for a three-phase system with a 200V magnitude for each phase. The inverter uses the same transformer for the PV array and wind turbine, increasing the output to 440V. In order to manage output generation, the fuel regulator block control the fuel flow. The block diagram of the fuel cell source [15] is depicted in Fig. 5.

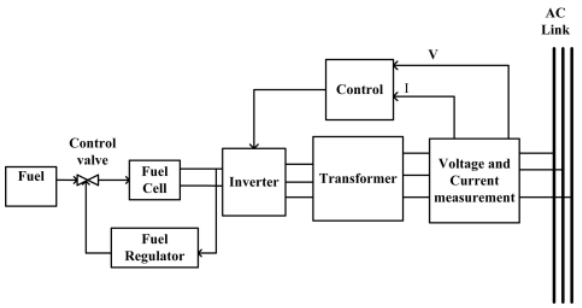


Fig. 5: Fuel cell source wing

D. Power stabilization

PID, FOPID, and SMC, have been modified using GA and GWO algorithms to reduce power fluctuations in three-generation sources, with an analysis identifying the best controller.

E. Optimization of controllers

The PID, FOPID, and SMC controllers have been optimized using GA and GWO techniques. Figure 6 block diagram depicts a closed-loop system with a direct-path PID controller, which is the typical relationship. The system's output would try its best to follow the reference signal, or setpoint. Three gains define the PID controller, as seen in Fig. 7.

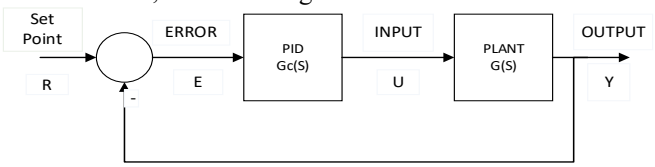


Fig. 6: PID control

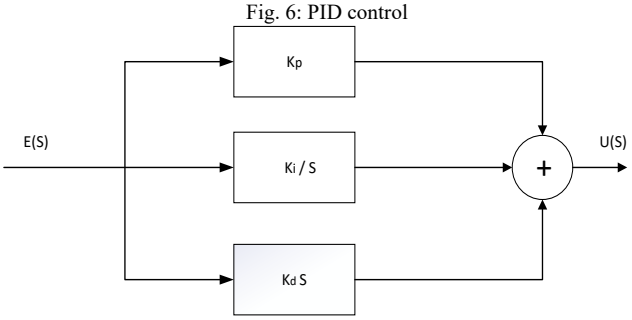


Fig. 7*:* PID Controller Internal Structure

The frequency domain expression of the connection between the output and input of a PID controller can be found in (1).

$$G_c(S) = \frac{U(S)}{E(S)} = K_p + \frac{k_i}{s} + k_d \qquad (1)$$

$G_c(s)$ is the transfer function, U(s) is the control variable, E(s) is the error value, K_p is proportional gain, K_i is the integral gain, K_d is derivative gain of the PID controller.

FOPID controller block diagram presented in Fig. 8, an application of fractional calculus, extends ordinary PID controller, offering greater flexibility and minimal control effort for accurate real-life operations. FOPID controllers, with two additional tuning parameters, outperform traditional PID controls in closed loop responses, offering greater resilience, adaptability, and less disturbance susceptibility in regulated plants. Transfer function for FOPID controller is depicted in (2).

$$G_{FOPID}(s) = \frac{U(s)}{E(s)} = K_p + \frac{K_i}{s^{\lambda}} + K_d s^{\mu}, (0 \leqslant \lambda, \mu \leqslant 2) \qquad (2)$$

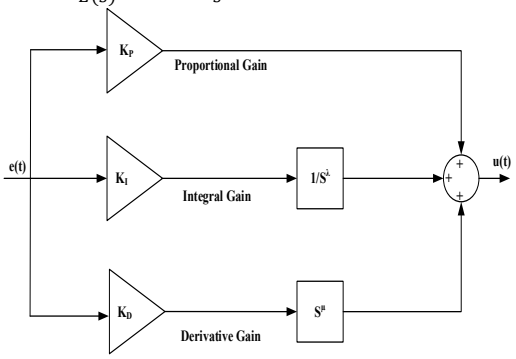


Fig. 8 FOPID controller

$G_{FOPID}(s)$ is the transfer function, U(s) is the control variable K_p is the proportional gain, K_i is the integral gain, K_d is the derivative gain, λ and μ are additional tuning knobs that would provide the benefit to the control loop.

Sliding mode control shown in Fig. 9 is widely used in systems due to its ease of use and resilience against external disturbances and uncertainties. It involves drawing system states into a specific region and creating control laws.

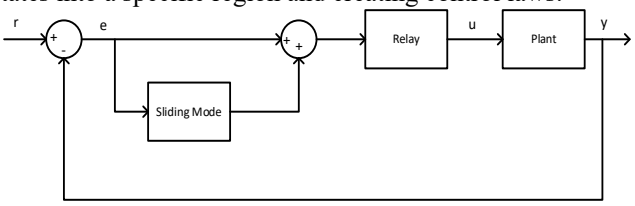


Fig. 9 Block diagram of SMC

Optimization strategies aim to reduce the cost function of the integral square error (ISE), a system performance measure used in optimal linear control and estimation theory typically makes use of this objective function.Eq.3 can be used to define ISE.

$$ISE = \int_0^{\infty} [e(t)]^2 dt \qquad (3)$$

Both optimizing algorithms have thirty iterations total with all controls. The Integral Square Error (ISE) serves as the goal function for all algorithms. Table I displays the values of the tuning parameters' upper and lower ranges for each algorithm [15].

Table I:
Limits on the advantages that can be achieved by every variant of PID

Gains	Lower Limit	Upper limit
K_p	880	1250
K_i	3750	4150
K_d	400	700
Λ	0.1	2
M	0.1	2

III. COMPUTATIONAL RESULTS AND DISCUSSION

The proposed nano-grid system effectively reduces power fluctuations due to various controllers (PID, FOPID and SMC) utilizing genetic algorithms and grey wolf optimization methods with fifty population size. A comparative study is conducted using graphical and tabular methods. The evolutionary algorithm optimizes all of these controllers, and the outputs of reactive and active power for the FOPID controller are displayed in Fig. 10 and 11.

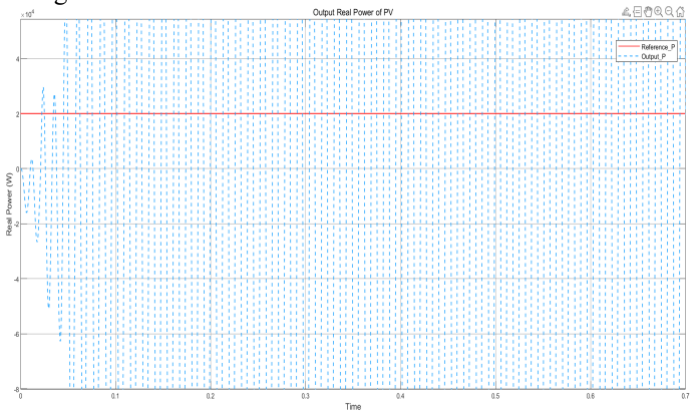


Fig. 10: FOPID Active Power result using GA

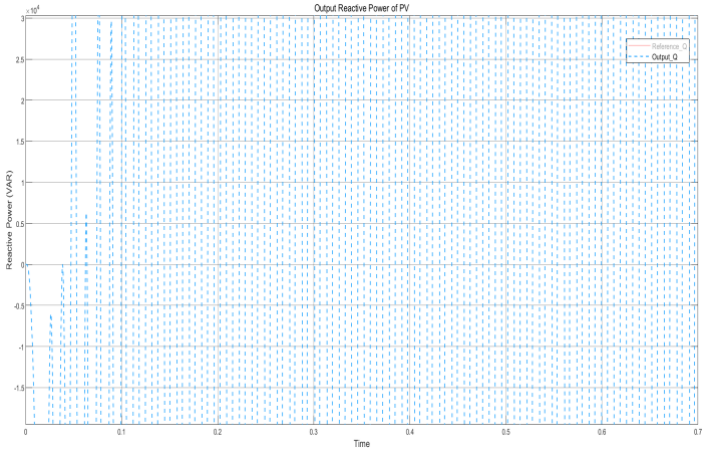


Fig. 11: FOPID Reactive Power result using GA

The outputs of reactive and active power for the PID controller are depicted in Fig. 12 and 13.

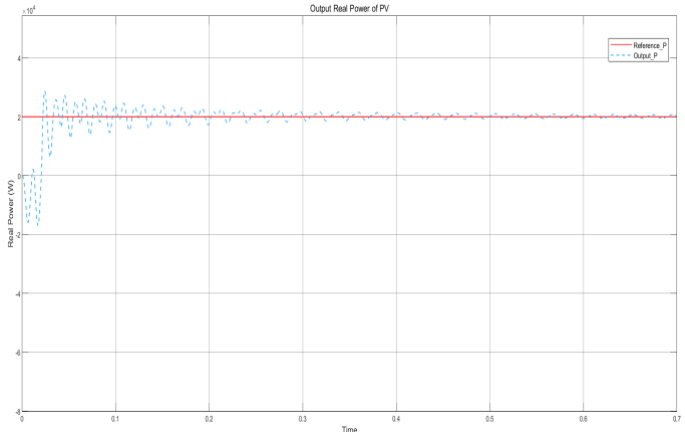


Fig. 12: PID Active Power result using GA

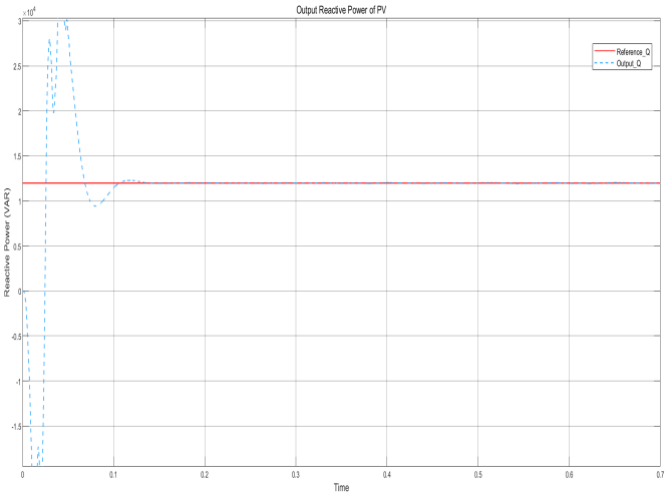


Fig. 13: PID Reactive Power result using GA

The outcomes of the SMC controller implemented with the Genetic Algorithm (GA) can be observed in below Fig.14 and Fig.15.

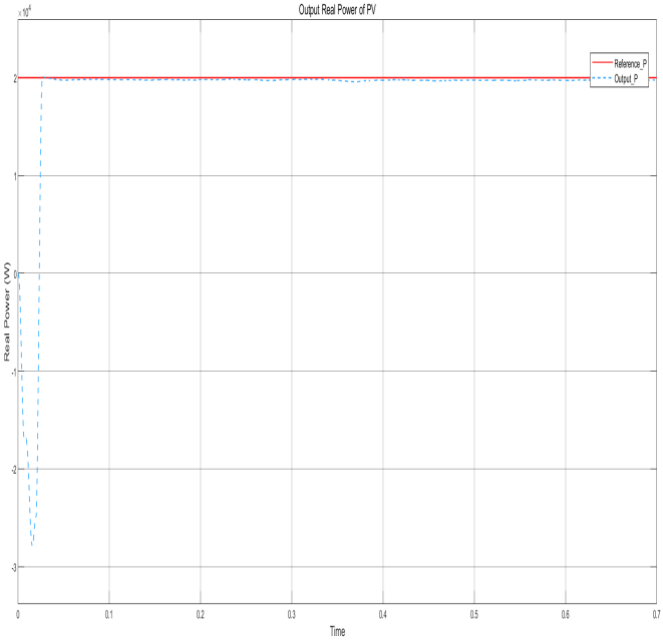


Fig. 14: SMC Active Power result using GA

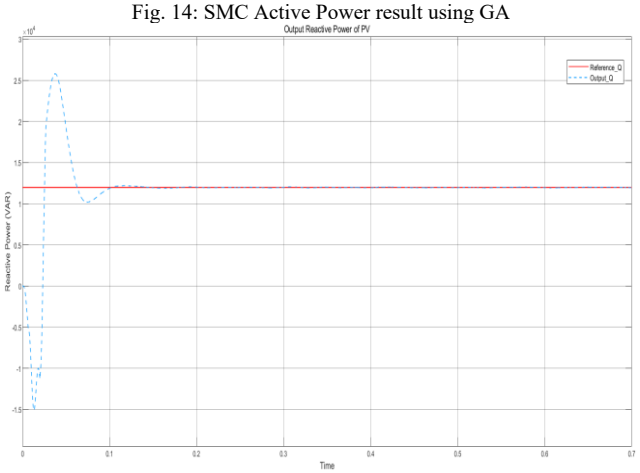


Fig. 15: SMC Reactive Power result using GA

Furthermore, it is worth mentioning that the outcomes obtained from optimizing the controllers using the genetic algorithm are nearly identical to those achieved using the GWO method. This is because the tuning parameters obtained using both approaches are very similar. Therefore, if the expansions of the controllers have comparable values, their answers will also be comparable. The combined results of active and reactive power with the genetic algorithm are shown in Fig. 16 and Fig. 17.

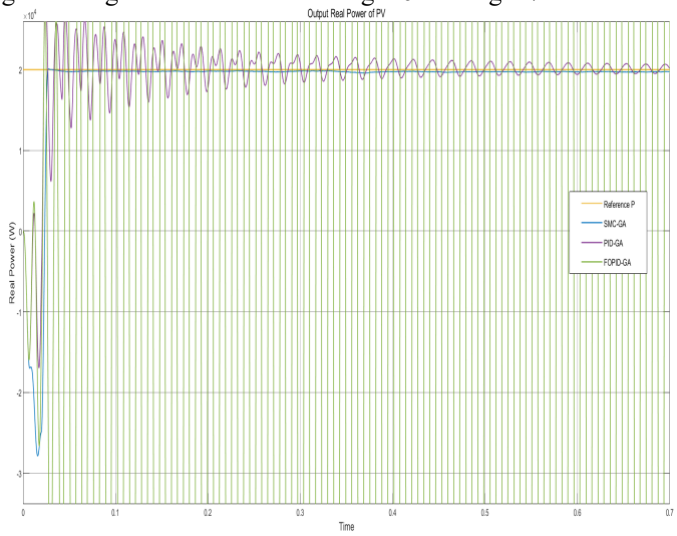


Fig. 16: SMC comparison using all GA optimized controllers (Active Power)

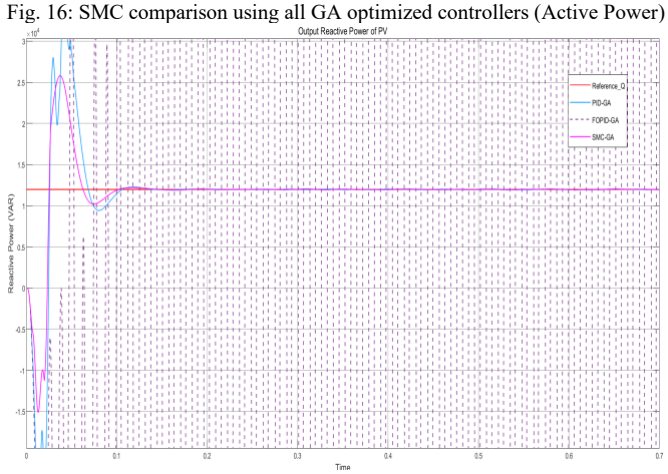


Fig. 17: SMC comparison using all GA optimized controllers (Reactive Power)

The FOPID-GA method has demonstrated the poorest performance, resulting in a notable steady-state inaccuracy. The performance of FOPID-GWO has proven to be superior to that of FOPID-GA. The optimized sliding mode control (SMC) controller has demonstrated exceptional efficacy in achieving power stabilization. Sliding Mode Control has therefore been included in the recommendation to regulate the power. Figures 18-23 show the results that were obtained by using GWO algorithms.

Combined results of active and reactive power of GWO are shown in Fig. 24 and Fig.25. Both techniques have produced identical gain values for the SMC controller. Note that GWO and GA algorithms behave similarly to most controllers for the proposed system. When pitted against the GA approach, the GWO algorithm has shown to be somewhat more effective.

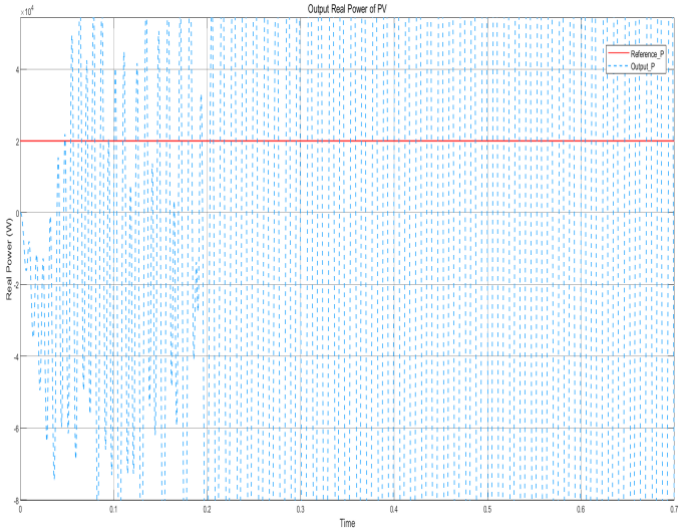


Fig. 18: FOPID Active Power result using GWO

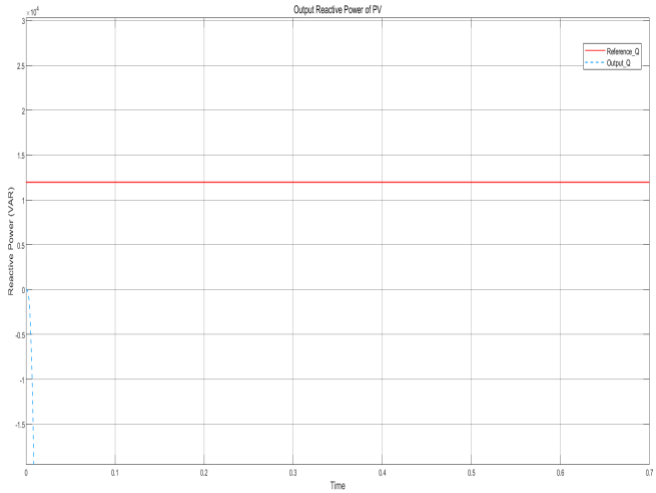


Fig. 19: FOPID Reactive Power result using GWO

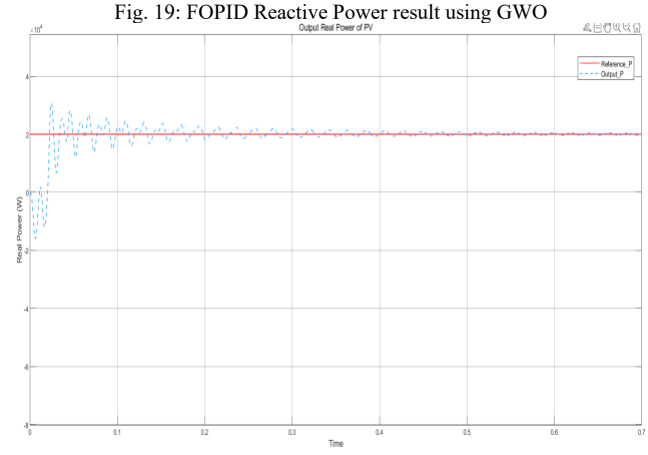


Fig. 20*:* Active Power result using GWO

System power fluctuations utilizing SMC with both techniques are determined to be negligible. Table II and III shows the gain values where every controller depicts the optimum power stability with respect to respective algorithm (GA & GWO). Table IV shows the evaluated time control parameters of every controller using GA and GWO.

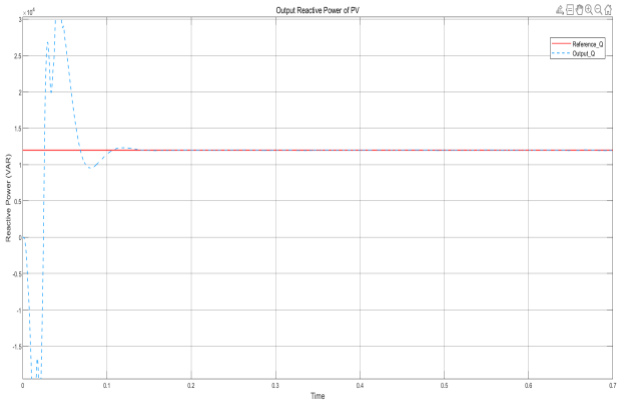


Fig. 21: PID Reactive Power result using GWO

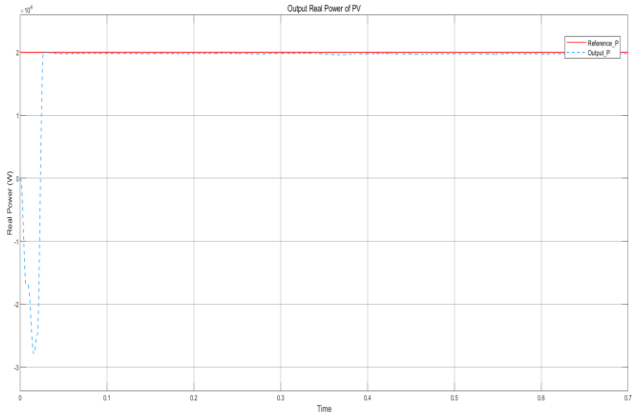


Fig. 22: SMC Active Power result using GWO

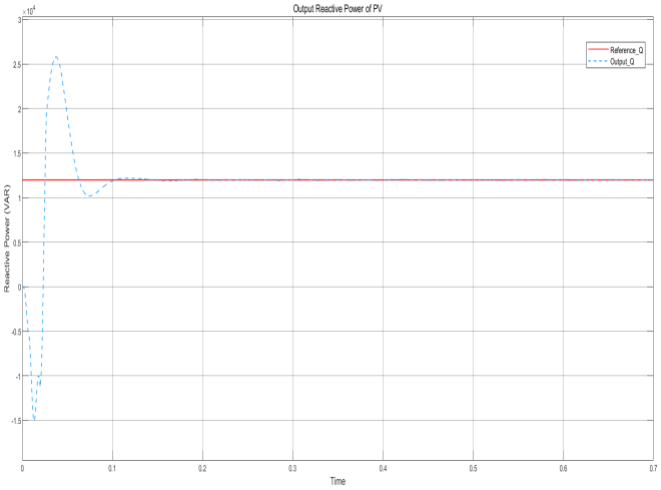


Fig. 23 SMC Reactive Power result using GWO

TABLE *II*: An evaluation and study of control parameters of number of different controllers using GA and GWO.

Controller	K_p	K_d	Ki	λ	μ
FOPID-GA	1194.8	567.71	3808.6	1.3991	0.96651
FOPID-GWO	1181.4	448.65	3860.4	1.3242	0.8928
PID-GA	902.06	526.87	3870.6	1	1
PID-GWO	1095.4	655.21	4044.5	1	1

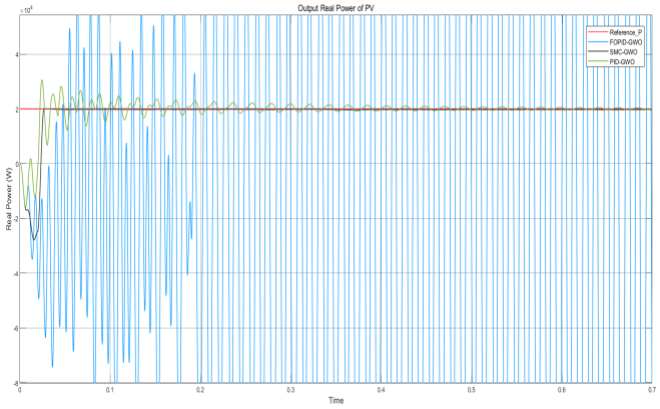


Fig. 24: SMC comparison using all GWO optimized controllers (Active Power)

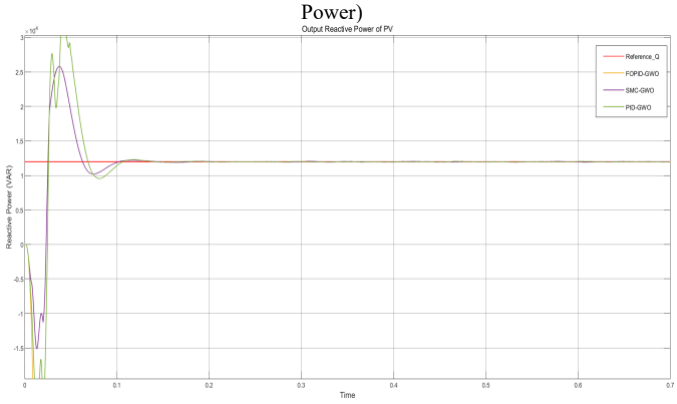


Fig. 25: SMC comparison using all GWO optimized controllers (Reactive Power)

TABLE *III*: An evaluation and study of control parameters of number of SMC controller using GA and GWO

Controller	Hysteresis band	Control action upper limit	Control action lower limit	Sample time
SMC	0.2	28	-28	-1

TABLE *IV*: An evaluation of time control parameters of number of different controllers using GA and GWO

Controller	Rise Time	Peak Time	Settling Time	Overshoot	Undershoot
GA-PID	0.0048	0.0247	0.4545	1.5286e+06	7.9726e+05
GWO-PID	0.0044	0.0246	0.4544	1.4680e+06	7.9674e+05
GA-FOPID	0.0025	0.6835	Non	9.4873e+06	1.4269e+07
GWO-FOPID	0.0017	0.6793	Non	9.1265e+06	1.2867e+07
SMC	0.0015	0.0159	0.0038	1.0047e+06	1.3938e+06

IV. CONCLUSION

SMC outperforms the optimized controller in achieving power stability. GWO algorithm outperforms the GA method, while FOPID controller is used. Analyzed the implementation

and performance indexes through the comprehensive analysis and graphical comparison of optimized controllers PID, FOPID and SMC using GA and GWO algorithms. Power quality is monitored within parameters, and the related load receives uninterrupted power in case of issues. An ideal renewable energy system is the most practical way to guarantee continuous power supply. An intelligent switching algorithm is used in a 60 KW system that combines fuel cell and renewable energy sources to connect the power supply source to the load. The GWO-tuned controller achieved quicker convergence, reduced overshoot, and a shorter settling time compared to the GA-tuned controller, which enhanced voltage and power stability. While the GA method also produced satisfactory outcomes, it required more computational resources and was slower in attaining the optimal controller parameters. Therefore, GWO is the more efficient and dependable tuning approach for this system, and future research could explore its application with hardware-in-the-loop validation and other hybrid metaheuristic strategies.

FUNDING STATEMENT

The author(s) received no specific funding for this study.

CONFLICTS OF INTEREST

The authors declare no conflicts of interest to report regarding the present study.

AUTHOR CONTRIBUTIONS

S.A., S.R., L.K., K.K., and R.S.: conceptualization, methodology, software, formal analysis, and writing of the original draft. M.K.L.B.: supervision, review and editing of the manuscript.

INSTITUTIONAL REVIEW BOARD STATEMENT

Not applicable. This study used only a public, anonymized dataset.

INFORMED CONSENT STATEMENT

Not applicable.

DATA AVAILABILITY STATEMENT

The dataset will be available upon reasonable request from the corresponding author.

DECLARATION OF GENERATIVE AI IN SCIENTIFIC WRITING

For preparing this manuscript, the authors have only made use of generative artificial intelligence systems to enhance language proficiency, grammar, and readability.

REFERENCES

[1] D. Sibtain, T. Rafiq, M. H. Bhatti, S. Shahzad, and H. Kilic, “Frequency stabilization for interconnected renewable based power system using cascaded model predictive controller with fractional order pad controller,” IET Renewable Power Generation, vol. 17, no. 16, pp. 3836–3855, 2023.

[2] S. Ali, M. Usman, S. Aziz, M. K. L. Bhatti, and S. Raza, “Analysis and simulation of optimized micro-grid,” Mehran University Research Journal of Engineering & Technology, vol. 41, no. 3, pp. 72–84, 2022.

[3] D. Dong, F. Luo, X. Zhang, D. Boroyevich, and P. Mattavelli, “Gridinterface bidirectional converter for residential DC distribution system Part 2: AC and DC interface design with passive components minimization,” IEEE Trans. Power Electron., vol. 28, no. 4, pp. 1667–1679, 2021.

[4] R. Ciavarella, G. Graditi, M. Valenti, A. Pinnarelli, G. Barone, M. Vizza, D. Menniti, N. Sorrentino, and G. Brusco, “Modeling of an energy hybrid system integrating several storage technologies: the dbs technique in a nanogrid application,” Sustainability, vol. 13, no. 3, p. 1170, 2021.

[5] M. Shahidehpour, Z. Li, W. Gong, S. Bahramirad, and M. Lopata, “A hybrid ac\/dc nanogrid: The keating hall installation at the illinois institute of technology.” IEEE Electrification Magazine, vol. 5, no. 2, pp. 36–46, 2017.

[6] B. Tudu, K. Mandal, and N. Chakraborty, “Optimal design and development of pv-wind-battery based nano-grid system: A fieldon-laboratory demonstration,” Frontiers in Energy, vol. 13, pp. 269–283, 2019.

[7] C. Cecati, H. A. Khalid, M. Tinari, G. Adinolfi, and G. Graditi, “Dc nanogrid for renewable sources with modular dc/dc llc converter building block,” IET Power Electronics, vol. 10, no. 5, pp. 536–544, 2017.

[8] K. D. Hoang and H.-H. Lee, “Accurate power sharing with balanced battery in distributed DC nano grid,” IEEE Transactions on Industrial Electronics, vol. 66, no. 3, pp.1883-1893,2019.

[9] M.M Rahman and J. pearce, “Modular open source solar photovoltaic-powered dc nano grids with efficient energy management system, “Solar Energy and Sustainable Development Journal, vol. 13, no. 1, pp.22-42,2024.

[10] I. Skouros and A. Karlis, “Design methodology of a dc nano grid incorporating the v2g technology,” in IECON 2019-45th Annual Conference of the IEEE Industrial Electronics Society, vol. 1. IEEE, 2019, pp. 5777–5782.

[11] A. K. Barik and D. C. Das, “Active power management of isolated renewable microgrid generating power from rooftop solar arrays, sewage waters and solid urban wastes of a smart city using salp swarm algorithm,” in 2018 Technologies for Smart-City Energy Security and Power (ICSESP). IEEE, 2018, pp. 1–6.

[12] Barik, Amar K., and Dulal C. Das. "Coordinated regulation of voltage and load frequency in demand response supported biorenewable cogeneration-based isolated hybrid microgrid with quasi-oppositional selfish herd optimisation." *International Transactions on Electrical Energy Systems* 30, no. 1, e12176, 2020.

[13] S. Kumar, V. Krishnasamy, S. Neeli, and R. Kaur, “Artificial intelligence power controller of fuel cell-based dc nano grid,” Renewable Energy Focus, vol. 34, pp. 120–128, 2020.

[14] S. A. G. K. Abadi, T. Khalili, S. I. Habibi, A. Bidram, and J. M. Guerrero, “Adaptive control and management of multiple nano-grids in an islanded dc microgrid system,” IET Generation, Transmission & Distribution, vol. 17, no. 8, pp. 1799–1815, 2023.

[15] S. Yousaf, A. Mughees, M. G. Khan, A. A. Amin, and M. Adnan, “A comparative analysis of various controller techniques for optimal control of smart nano-grid using ga and pso algorithms,” IEEE Access, vol. 8, pp. 205 696–205 711, 2020.

[16] Babary, Saad Rehman, and Ramsha Khalid. "Leveraging Transformer-Based Natural Language Processing for Adaptive Language Learning in Digital Humanities Environments." *Journal of Artificial Intelligence and Computing* 4, no. 1, 36-43, 2026.

[17] Younas, Muhammad Hammad, and Irshad Ahmed Sumra. "Governing Artificial Intelligence by Standard and by Statute: A Comparative Review of ISO/IEC 42001 and the EU Artificial Intelligence Act." *Journal of Artificial Intelligence and Computing* 4, no. 1, 56-64, 2026.

[18] Naseer, Fawad, Muhammad Nasir Khan, Abdullah Addas, Qasim Awais, and Nafees Ayub. "Game mechanics and artificial intelligence personalization: A framework for adaptive learning systems." *Education Sciences* 15, no. 3, 301, 2025.

[19] Jamil, Mohsin, Asim Waris, Syed Omer Gilani, Bilal A. Khawaja, Muhammad Nasir Khan, and Ali Raza. "Design of robust higher-order repetitive controller using phase lead compensator." *IEEE Access* 8, 30603-30614, 2020.